

CTEQ TEA PDF Analysis: new experimental data and constraints on new physics

Marco Guzzi

Southern Methodist University, Dallas, TX

Pheno 2010 - Univ. of Wisconsin-Madison

Based on the papers:

- 1) New Global PDF Analysis and Light Gluinos: Tools for the LHC
-E.Berger, M.G., H.L. Lai, F. Olness and P. Nadolsky-
- 2)CTEQ 2010 paper

Two questions are addressed in this talk:

1. *What is the impact of the combined HERA Run I data on the CTEQ analysis?*
2. *Can the new data better constrain non-SM physics?*

Example:

- PDF fits with experimental α_s constraints.
- Constraints on color-octet fermions (SUSY-like gluinos) from the global hadronic data.

I will show a selection of figures.

Additional figures are in the PDF file as “Backup” slides!

Two questions are addressed in this talk:

1. What is the impact of the combined HERA Run I data on the CTEQ analysis?

Changes in the central Fits: PDF's Ratio, $Q = 2 \text{ GeV}$

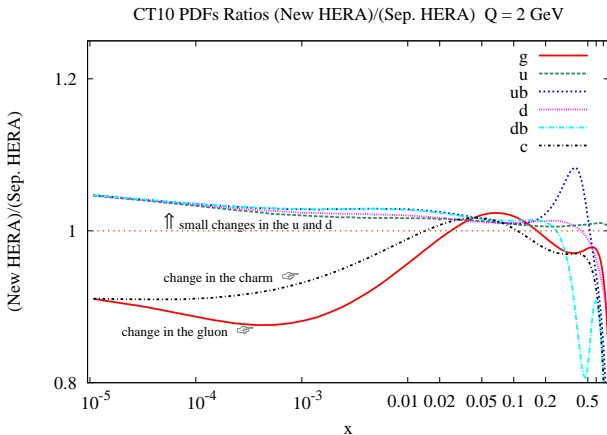
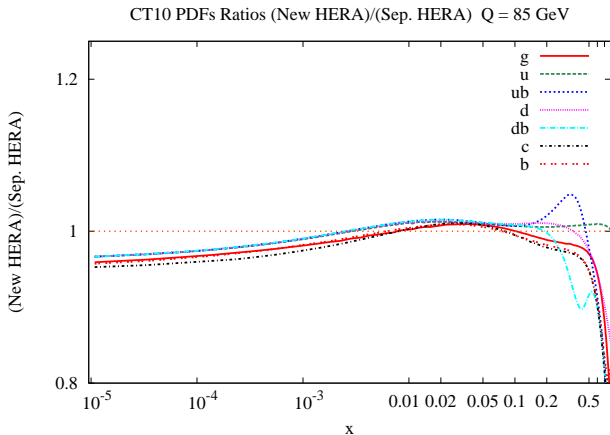


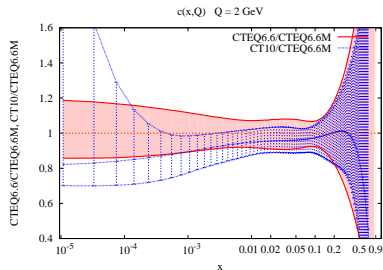
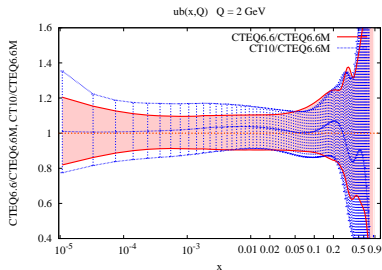
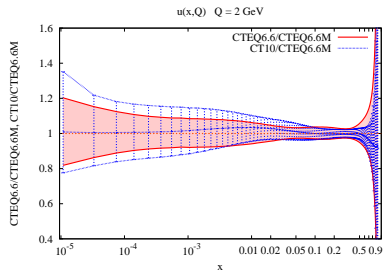
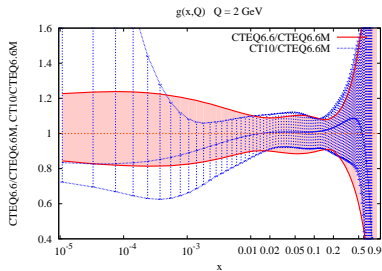
Figure: PDF Ratios: (CT10 with the new HERA Run I data vs (CT10 with the separate HERA data)) for $Q = 2 \text{ GeV}$.

Changes in the central Fits: PDF's Ratio, $Q = 85$ GeV



Smaller changes at 85 GeV

New HERA Run-I data: CT10 vs CTEQ6.6.



The Impact of HERA data on the PDF uncertainty, Gluon

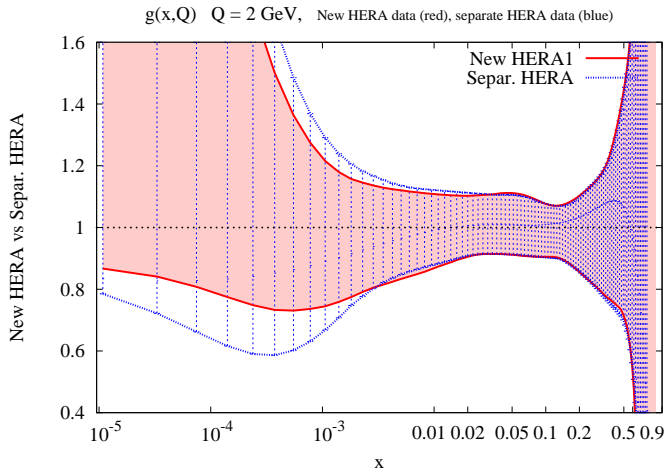


Figure: Error bands: (red) CT10 new HERA Run I data, (blue) CT10 with the separate HERA data. $g(x)$, $Q = 2 \text{ GeV}$.

Applications for the Hadron Colliders:

2. Can the global analysis constrain new physics?

Consider for instance **gluinos**
from **supersymmetry**.

Bounds

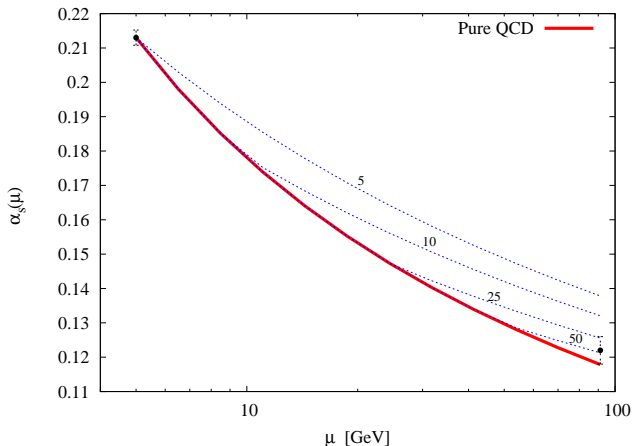
Current bounds: are relatively light, 10-50 GeV depending on how much trust is put in the constraints from *LEP* events shapes.

Can we improve on these?

(See also Berger, Nadolsky, Olness and Pumplin PRD71 2004, Blümlein and Botts PLB325 1994, Rückl and Vogt Z.Phys.64 1994)

Running of α_s in SM and SUSY

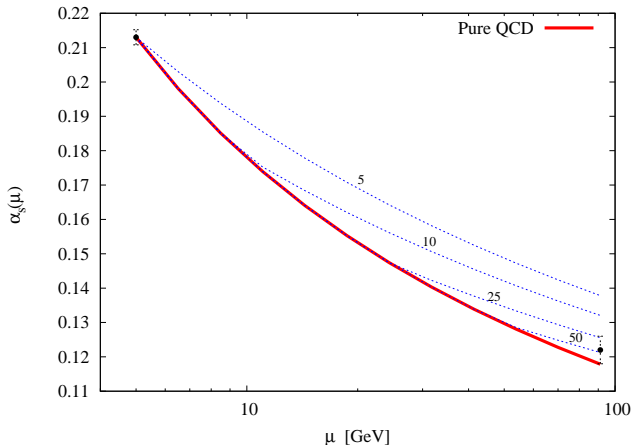
$$m_{\tilde{g}} = 5, 10, 25, 50 \text{ GeV}$$



The most accurate constraints on α_s reside at $Q < 10$ GeV and $Q = M_Z$.
Running of α_s from $Q = 10$ GeV to M_Z may reveal non-SM physics.

Running of α_s in SM and SUSY

$$m_{\tilde{g}} = 5, 10, 25, 50 \text{ GeV}$$

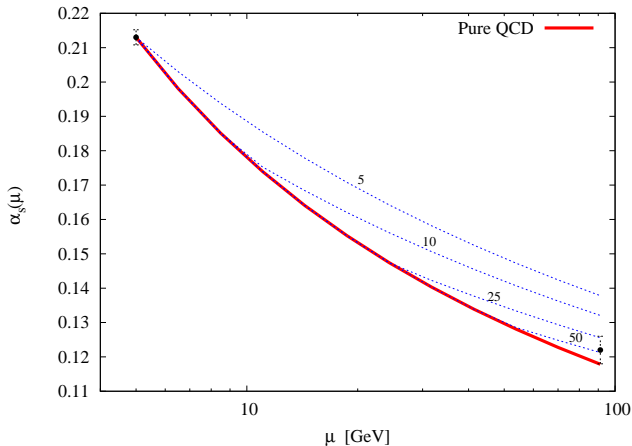


New feature \Rightarrow

In the fits we have introduced $\alpha_s(M_Z)$ as a fitting parameter.

Running of α_s in SM and SUSY

$m_{\tilde{g}} = 5, 10, 25, 50$ GeV

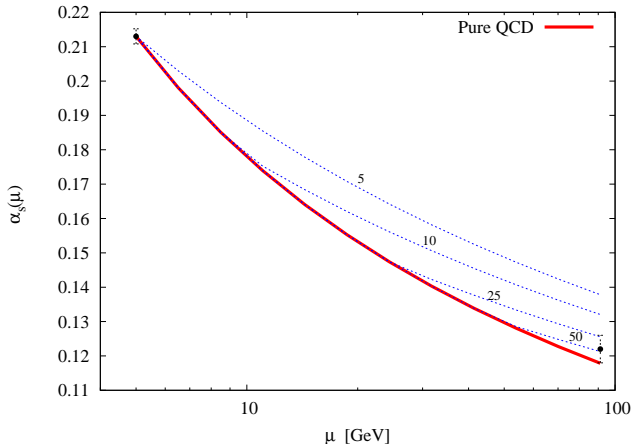


We have included the following data:

a) **The hadronic data**

Running of α_s in SM and SUSY

$$m_{\tilde{g}} = 5, 10, 25, 50 \text{ GeV}$$

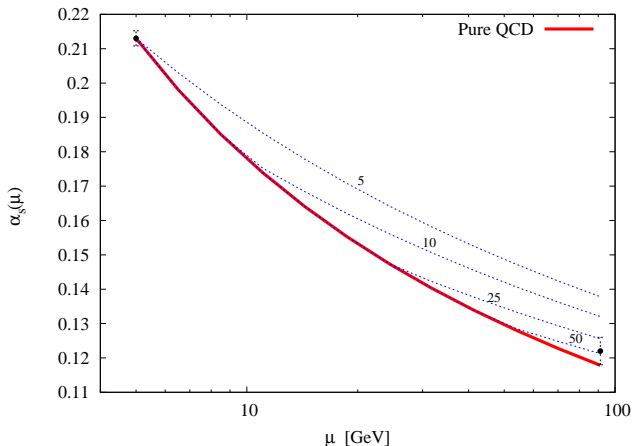


We have included the following data:

b) $\alpha_s(M_Z) = 0.123 \pm 0.0040$ from $e^+ e^-$ hadronic event shapes (see Dissertori *et al.*)

Running of α_s in SM and SUSY

$$m_{\tilde{g}} = 5, 10, 25, 50 \text{ GeV}$$



We have included the following data:

c) a lower- Q composite constraint at $Q = 5$ GeV

$$\alpha_s(Q) = 0.213 \pm 0.0022$$

Composite α_s at $Q = 5 \text{ GeV}$

$$\alpha_s(Q = 5 \text{ GeV}) = 0.213 \pm 0.002$$

- Obtained by the combination of

$$\alpha_s(Q = 5) = 0.218612 \pm 0.005757$$

from τ decay (see Baikov, Chetyrkin, Kuhn PRL101 2008)

(1)

$$\alpha_s(Q = 5) = 0.21435 \pm 0.00301$$

from heavy quarkonia (see Amsler *et. al.* PLB667 2008 ref. therein)

(2)

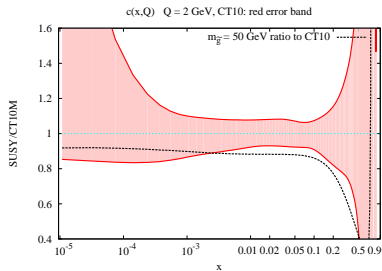
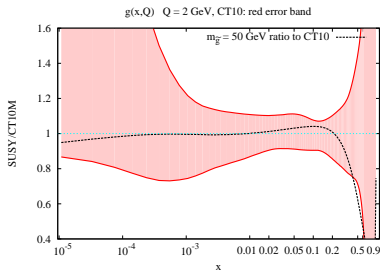
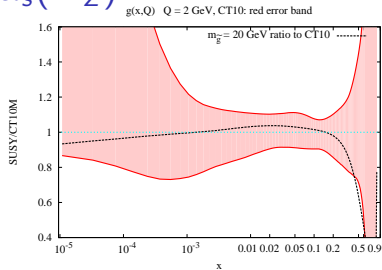
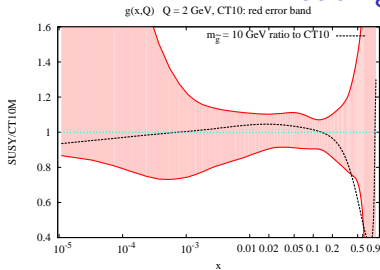
$$\alpha_s(Q = 5) = 0.20897 \pm 0.003925$$

from lattice QCD (see Amsler *et. al.* PLB667 2008)

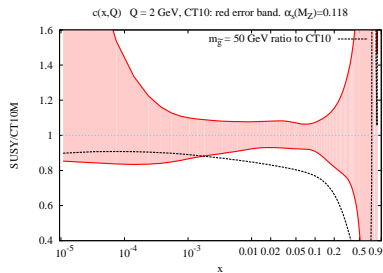
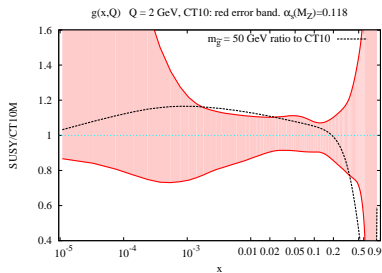
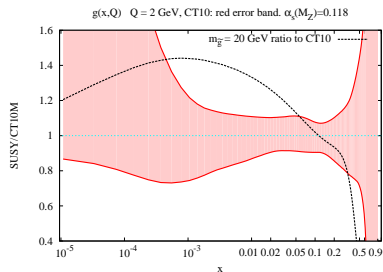
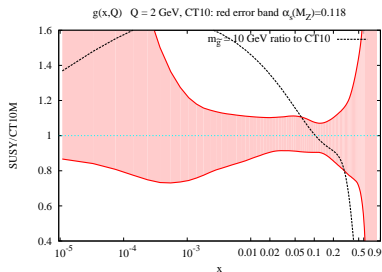
(3)

- Evolved to the common scale $Q = 5 \text{ GeV}$ in pure QCD and added as a weighted mean.

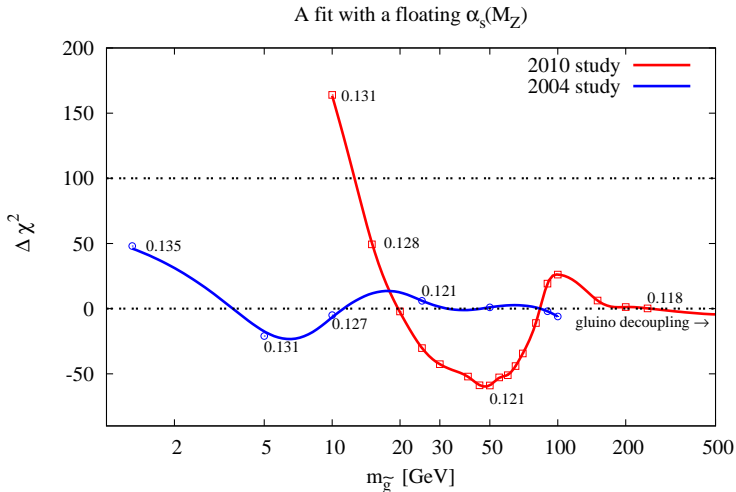
The impact of gluinos on the PDFs: floating $\alpha_s(M_Z)$



The impact of gluinos on the PDFs: $\alpha_s(M_Z) = 0.118$



$\Delta\chi^2$ as a function of $m_{\tilde{g}}$: Floating $\alpha_s(M_Z)$

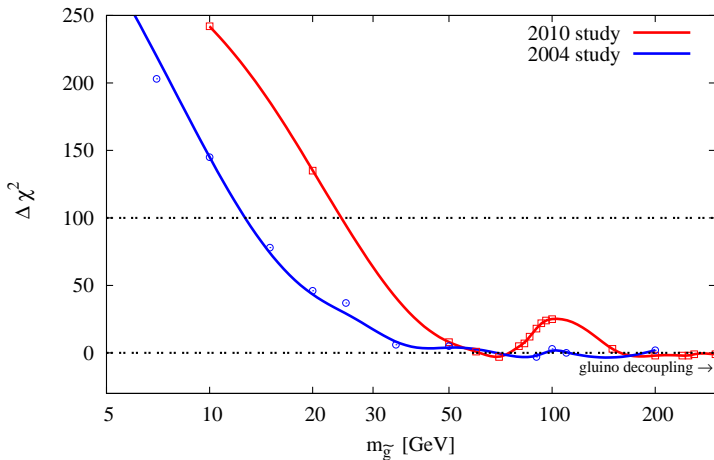


$m_{\tilde{g}} < 15$ GeV are excluded for all the $\alpha_s(M_Z)$ values.

$m_{\tilde{g}} \approx 50$ GeV results in $\Delta\chi^2 \approx -55$ as compared to the pure QCD case

$\Delta\chi^2$ as a function of $m_{\tilde{g}}$: Fixed $\alpha_s(M_Z) = 0.118$

A fit with a fixed $\alpha_s(M_Z)=0.118$



$m_{\tilde{g}} < 25$ GeV are excluded for the fits with a fixed $\alpha_s(M_Z)$.

There is an improvement with respect to the study performed in 2004

Why are the constraints on gluinos remain weak?

- Precise DIS data are at $Q < 20 - 30 \text{ GeV} \Rightarrow$ cannot constrain heavier gluinos.
- In the jet data, the reduction in the NLO rate due to suppressed gluon PDF is compensated by a larger α_s .
- At the LHC, $\sqrt{S} = 7 \text{ TeV}$ the discovery of gluino-like fermions could be feasible with sufficient control on the systematic uncertainties and with precise measurements of α_s .

LHC@7 TeV: a fit with a fixed $\alpha_s(M_Z) = 0.118$

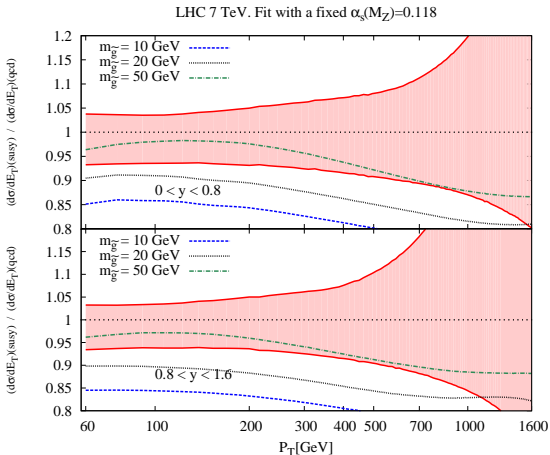


Figure: Ratios between the cross sections computed for $m_{\tilde{g}} = 10, 20, 50$ GeV and **CT10 prel.** for the LHC at 7 TeV.

LHC@7 TeV: a fit with a floating $\alpha_s(M_Z)$

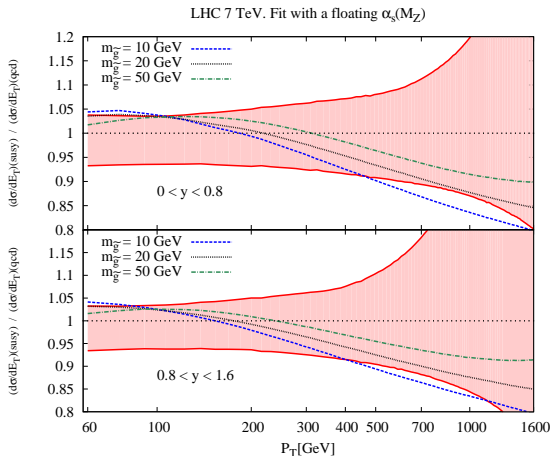


Figure: Ratios between the cross sections computed for $m_{\tilde{g}} = 10, 20, 50 \text{ GeV}$ and **CT10 preL** for the LHC at 7 TeV.

LHC@14 TeV: a fit with a fixed $\alpha_s(M_Z) = 0.118$

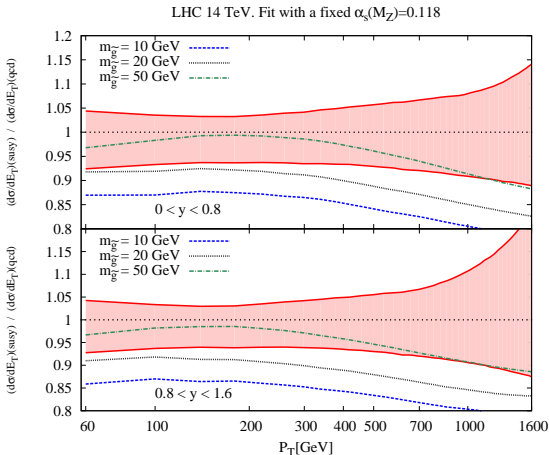


Figure: Ratios between the cross sections computed for $m_{\tilde{g}} = 10, 20, 50$ GeV and **CT10 prel.** for the LHC at 14 TeV.

LHC@14 TeV: a fit with a floating $\alpha_s(M_Z)$

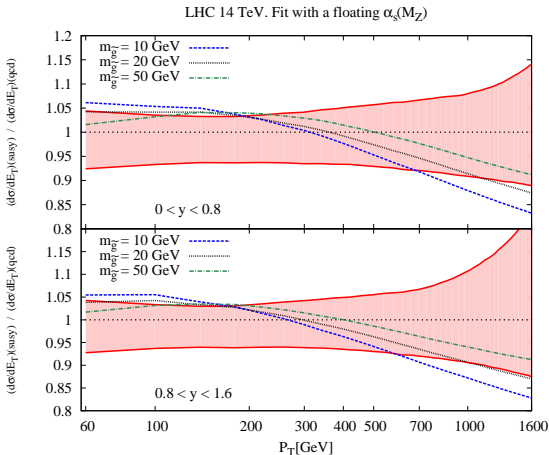


Figure: Ratios between the cross sections computed for $m_{\tilde{g}} = 10, 20, 50 \text{ GeV}$ and **CT10 prel.** for the LHC at 14 TeV.

Main Messages

- The combined HERA data improve constraints on the gluon PDF and the charm, and have a small impact on light-quark PDFs
- Some fits of the CT10 family include α_s measurements as the input data.
- PDF's with light gluino for the LHC measurements are available. Improvement in the χ^2 behaviour for $m_{\tilde{g}} = 50$ GeV is observed (Fits with a floating α_s).
- The new data provide substantial improvements in constraining models with gluinos lighter than 20 GeV.

Backup Slides

Introduction

New data are flowing in

- *Tevatron Run II inclusive Jet Production and W asymmetry (see Aaltonen et.al. PRD78 2008, Abulencia et.al. PRD75 2007, Abaov et. al. PRL101 2008)*
- *Precise HERA DIS data (see H1 and ZEUS Coll. JHEP1001 2010) with greatly reduced systematic uncertainties*
- *Forthcoming first LHC data*

We will examine changes in the CTEQ PDFs resulting from these data

Motivations for a new analysis

- *The recent current assets of new data from **Tevatron Run II** and from the very precise measurements of **HERA I** naturally motivate for a new analysis of the PDFs.*
In particular, those pose the problem of updating the present constraints on some observables solely determined by hadronic interactions.
- *The fact that the **Tevatron Run II** jet data are very “sensitive” to the gluon, rises the question on how big is the impact of the new **HERA I** data on the PDFs uncertainty and pushes to explore the kinematic domains in which the effects are relevant, in particular at small- x .*

Results From the Global Fits: Uncertainties

The uncertainty is computed by using the formula for the asymmetric errors (see Nadolsky and Sullivan 2001) in the positive and negative directions in the space of the PDF parameters

$$\delta^+ f = \sqrt{\sum_{i=0}^{N_{eigv}} \left[\max \left(f_0 - f_i^{(+)}, f_0 - f_i^{(-)}, 0 \right) \right]^2}$$

$$\delta^- f = \sqrt{\sum_{i=0}^{N_{eigv}} \left[\max \left(f_i^{(+)} - f_0, f_i^{(-)} - f_0, 0 \right) \right]^2}, \quad (4)$$

where f is the generic PDF, f_0 is the central value, N_{eigv} is the number of the eigenvectors considered, while f^\pm are the positive and negative variations of f respectively, computed in the space of the PDF parameters. The error band are normalized as

$$\Delta^{(+)} f(x) = \frac{f + \delta^+ f}{f} \quad \Delta^{(-)} f(x) = \frac{f - \delta^- f}{f} \quad (5)$$

The Impact of HERA data on the PFD uncertainty, Charm

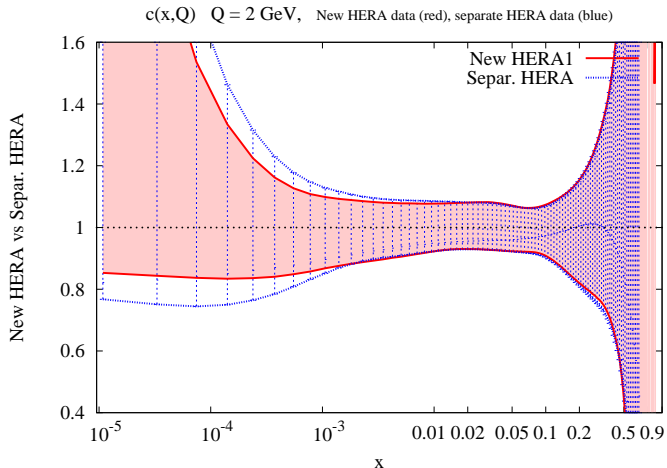
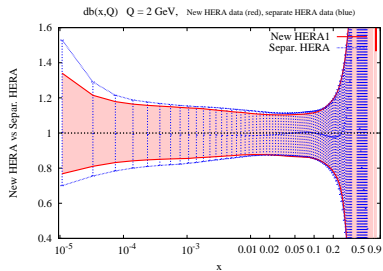
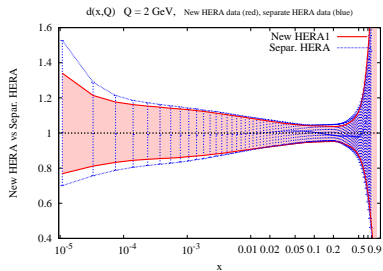
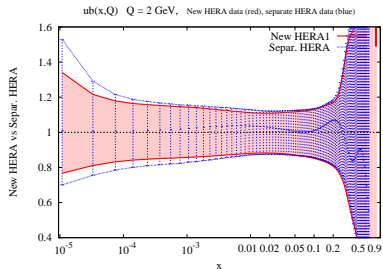
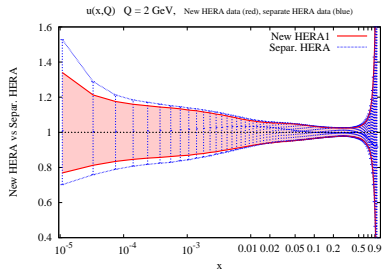
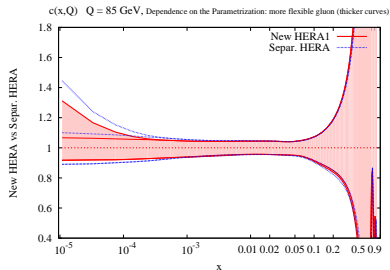
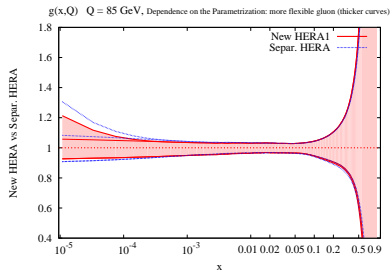
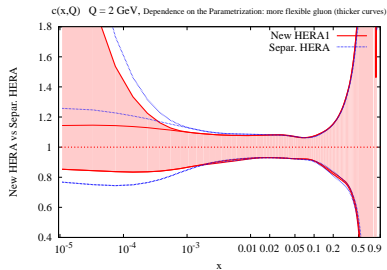
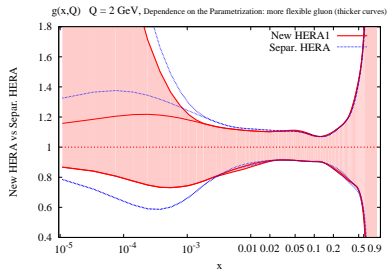


Figure: Error bands: (red) CT10 new HERA Run I data, (blue) CT10 with the separate HERA data. $c(x)$, $Q = 2 \text{ GeV}$.

u, \bar{u}, d, \bar{d}


Sensitivity of the fits to the parametrizations



Results From the Global Fits: Ratios within the error band,

$$Q = 2 \text{ GeV}$$

(New HERA)/(Sep. HERA): $g(x)$ red band, $c(x)$ blue band $Q = 2 \text{ GeV}$

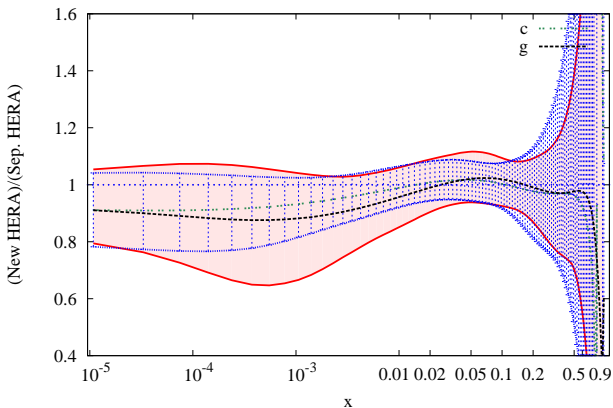


Figure: Ratios of **CT10** with the new HERA data and with the separate HERA data for the gluon and the charm within the respective error bands for $Q = 2 \text{ GeV}$.

Results From the Global Fits: Ratios within the error band,

$$Q = 85 \text{ GeV}$$

(New HERA)/(Sep. HERA): g(x) red band, c(x) blue band $Q = 85 \text{ GeV}$

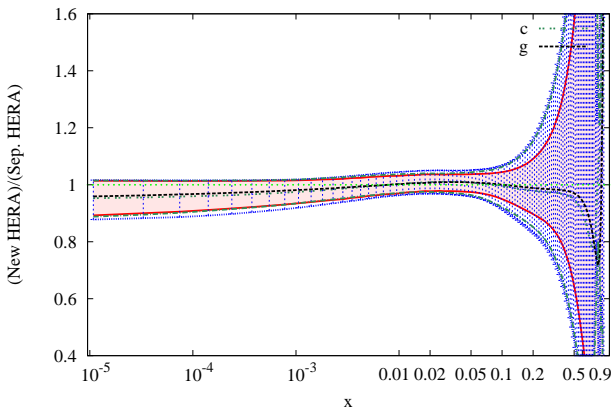


Figure: Ratios of **CT10** with the new HERA data and with the separate HERA data for the gluon and the charm within the respective error bands for $Q = 85 \text{ GeV}$.

Fit modifications due to the gluino

Glueinos modify the fits in three ways:

- 1 The gluino alters $\alpha_s(Q)$, thereby modifying the evolution of ordinary quark and gluon PDFs.

$$\begin{aligned}
 Q \frac{\partial}{\partial Q} \alpha_s(Q) &= -\frac{\alpha_s^2}{2\pi} \sum_{n=0}^{\infty} \beta_n \left(\frac{\alpha_s}{4\pi}\right)^n \\
 &= -\left[\beta_0 \frac{\alpha_s^2}{2\pi} + \beta_1 \frac{\alpha_s^3}{2^3 \pi^2} + \dots \right].
 \end{aligned} \tag{6}$$

$$\beta_0 = 11 - \frac{2}{3} n_f - 2n_{\tilde{g}} - \frac{1}{6} n_{\tilde{f}}, \tag{7}$$

$$\beta_1 = 102 - \frac{38}{3} n_f - 48n_{\tilde{g}} - \frac{11}{3} n_{\tilde{f}} + \frac{13}{3} n_{\tilde{g}} n_{\tilde{f}}, \tag{8}$$

Fit modifications due to the gluino

Gluinos modify the fits in three ways:

- 2 DGLAP equations are extended to account for the new processes:

$$Q^2 \frac{d}{dQ^2} \begin{pmatrix} \Sigma(x, Q^2) \\ g(x, Q^2) \\ \tilde{g}(x, Q^2) \end{pmatrix} = \frac{\alpha_s(Q^2)}{2\pi} \times$$

$$\times \int_x^1 \frac{dy}{y} \begin{pmatrix} P_{\Sigma\Sigma}^{NLO}(x/y) & P_{\Sigma\tilde{g}}^{NLO}(x/y) & P_{\Sigma\tilde{g}}^{LO}(x/y) \\ P_{g\Sigma}^{NLO}(x/y) & P_{g\tilde{g}}^{NLO}(x/y) & P_{g\tilde{g}}^{LO}(x/y) \\ P_{\tilde{g}\Sigma}^{LO}(x/y) & P_{\tilde{g}g}^{LO}(x/y) & P_{\tilde{g}\tilde{g}}^{LO}(x/y) \end{pmatrix} \begin{pmatrix} \Sigma(y, Q^2) \\ g(y, Q^2) \\ \tilde{g}(y, Q^2) \end{pmatrix} \quad (6)$$

$$\Sigma(x, Q^2) = \sum_{i=u,d,s,\dots} (q_i(x, Q^2) + \bar{q}_i(x, Q^2)). \quad (7)$$

$\Sigma(x, Q^2)$, $g(x, Q^2)$, and $\tilde{g}(x, Q^2)$ are the singlet quark, gluon, and gluino PDFs. At $10^{-5} < x < 1$, $\tilde{g}(x, Q^2) \ll g(x, Q^2)$ and $\tilde{g}(x, Q^2) \ll q(x, Q^2)$. We include the gluino terms in splitting functions at *LO*, without sacrificing the overall NLO accuracy of the whole fit.

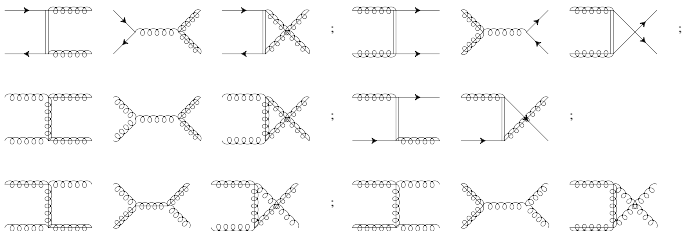
Fit modifications due to the gluino

Glueinos modify the fits in three ways:

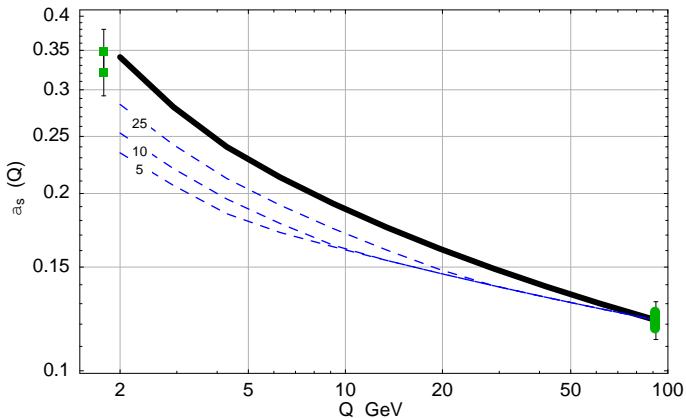
- 3 Glueinos contribute to some hard scattering processes

⇒ In DIS and vector boson production gluino hard scattering terms are of order $O(\alpha_s^2)$ → can be currently neglected

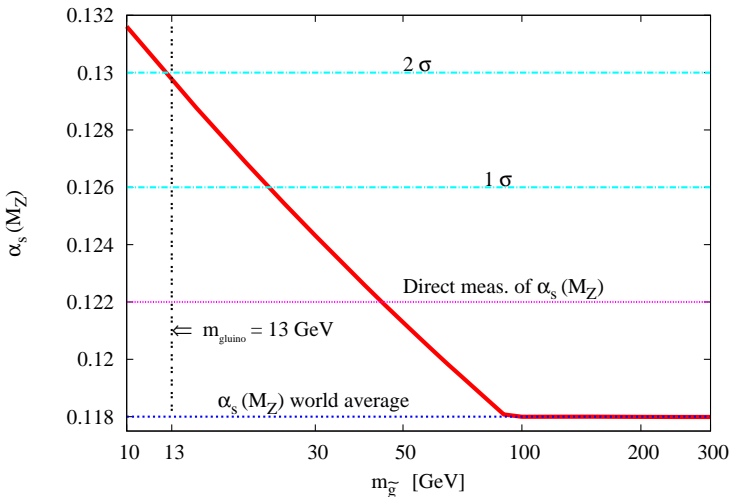
⇒ In jet production, LO gluino terms with massive kinematics are included (see Backup slides)



Running $\alpha_s(M_Z)$ as a function of $m_{\tilde{g}}$: from high scale to low scale



$\alpha_s(M_Z)$ as a function of $m_{\tilde{g}}$



$m_{\tilde{g}} < 50$ GeV can be accommodated only with
 $\alpha_s = 0.122 - 0.130$.

Computation of the Jet cross sections for massive kinematics

The energy flowing in the s channel at parton level is given by

$$\hat{s} = (p_1 + p_2)^2 = (p_3 + p_4)^2 = 2p_1 \cdot p_2 = 2m_{\bar{g}}^2 + 2p_3 \cdot p_4. \quad (9)$$

We introduce the transverse momentum $p_T = |\vec{p}| \sin \theta$, where θ is the scattering angle, the transverse mass m_T , and the rapidity as follows

$$\begin{aligned} p_3^\mu &= (m_{T,3} \cosh y_3, p_{T,3} \sin \phi, p_{T,3} \cos \phi, m_{T,3} \sinh y_3), \\ p_4^\mu &= (m_{T,4} \cosh y_4, p_{T,4} \sin \bar{\phi}, p_{T,4} \cos \bar{\phi}, m_{T,4} \sinh y_4), \\ m_{T,3}^2 &= p_{T,3}^2 + m_{\bar{g}}^2, \quad m_{T,4}^2 = p_{T,4}^2 + m_{\bar{g}}^2, \\ y_3 &= \frac{1}{2} \ln \left(\frac{E_3 + p_{z,3}}{E_3 - p_{z,3}} \right). \end{aligned} \quad (10)$$

Here ϕ is the azimuthal angle and in a back-to-back production $\phi - \bar{\phi} = \pi$. We also introduce the transverse energy of a jet that we defined as $E_T = E \sin \theta$, where $E = \sqrt{|\vec{p}|^2 + m^2}$.

Computation of the Jet cross sections for massive kinematics

The Lorentz invariant phase space for two particles in the final state is given by

$$\begin{aligned}
 d\text{PS}_2 &= \frac{d^2\vec{p}_{T_3}}{(2\pi)^3} \frac{d|\vec{p}_{T_3}|}{2} \delta\left(\sqrt{m_{T_3}^2 - m_g^2} - |\vec{p}_{T_3}|\right) dy_3 \\
 &\times \frac{d^2\vec{p}_{T_4}}{(2\pi)^3} \frac{d|\vec{p}_{T_4}|}{2} \delta\left(\sqrt{m_{T_4}^2 - m_g^2} - |\vec{p}_{T_4}|\right) dy_4 \times (2\pi)^4 \delta^{(2)}(\vec{p}_{T_3} + \vec{p}_{T_4}) \\
 &\delta\left((x_1 + x_2)\sqrt{S}/2 - p_3^0 - p_4^0\right) \delta\left((x_1 - x_2)\sqrt{S}/2 - p_3^3 - p_4^3\right).
 \end{aligned}
 \tag{11}$$

The differential cross section

The differential cross section expressed in terms of the transverse momenta and of the rapidities is finally given by

$$\frac{d\sigma}{d\vec{p}_{T_3} d\vec{p}_{T_4} dy_3 dy_4} = \frac{1}{16\pi^2 S^2} \frac{f_{H_1 \rightarrow 1}(x_1, \mu_F^2)}{x_1} \frac{f_{H_2 \rightarrow 2}(x_2, \mu_F^2)}{x_2} \times \sum |\mathcal{M}_{p_1 p_2 \rightarrow p_3 p_4}|^2 \delta^{(2)}(\vec{p}_{T_3} + \vec{p}_{T_4}) \quad (12)$$

where the parton fractions are

$$x_1 = \frac{m_{T_3}}{\sqrt{S}} e^{y_3} + \frac{m_{T_4}}{\sqrt{S}} e^{y_4}, \quad x_2 = \frac{m_{T_3}}{\sqrt{S}} e^{-y_3} + \frac{m_{T_4}}{\sqrt{S}} e^{-y_4} \quad (13)$$

Integrating out \vec{p}_{T_4} over the two dimensional Dirac delta we obtain

$$\frac{d\sigma}{dp_T dy_3 dy_4} = \frac{p_T}{8\pi S^2} \frac{f_{H_1 \rightarrow 1}(x_1, \mu_F^2)}{x_1} \frac{f_{H_2 \rightarrow 2}(x_2, \mu_F^2)}{x_2} \sum |\mathcal{M}_{p_1 p_2 \rightarrow p_3 p_4}|^2 \quad (14)$$

where $p_T = |\vec{p}_{T_3}|$, $x_1 = m_T/\sqrt{S}(e^{y_3} + e^{y_4})$, $x_2 = m_T/\sqrt{S}(e^{-y_3} + e^{-y_4})$, and $m_T^2 = p_T^2 + m_{\tilde{g}}^2$.